

Exponential Tails in the Centroid Velocity Distributions of Star-Forming Regions

Mark S. Miesch

Joint Institute for Laboratory Astrophysics
and Department of Astrophysical, Planetary, and Atmospheric Sciences
University of Colorado – Campus Box 440 Boulder, CO 80309
miesch@solarz.colorado.edu

and

John M. Scalo

Department of Astronomy
University of Texas at Austin Austin, TX 78712
parrot@astro.as.utexas.edu

(a shorter version) Submitted to the Astrophysical Journal Letters
Draft date: Dec. 1, 1994

Subject headings: ISM: clouds, ISM: molecules, stars: formation, turbulence

ABSTRACT

Probability density functions (pdfs) of ^{13}CO emission line centroid (line-of-sight, intensity-weighted average) velocities are presented for several densely sampled molecular clouds as quantitative descriptors of their underlying dynamics. Although some are approximately Gaussian in form, most of the pdfs exhibit relatively broader, often nearly exponential, tails, similar to the pdfs of velocity *differences* and *derivatives* (but not the velocity field itself) found in experiments and numerical simulations of incompressible turbulence. The broad pdf tails found in the present work are also similar to those found in decades-old measurements of interstellar velocity pdfs using atomic line centroids, and to the excess wing emission recently found in individual molecular line profiles. Some possible interpretations of the observed deviations are briefly discussed, although none of these account for the nearly exponential tails.

1. Introduction

Although a great deal of effort has been devoted to quantitatively describing the complex spatial structure of star-forming regions (for recent approaches see Falgarone and Phillips 1990, 1991, Gill and Henriksen 1991, Langer, Wilson and Anderson 1993, Wiseman and Adams 1994a,b, Zimmermann and Stutzki 1994, Houlahan and Scalo 1992, Scalo 1990, Chappell and Scalo 1994), comparatively little attention has been paid to characterizing the radial velocity dimension of the data except for studies of possible velocity dispersion-size scaling relations (see Falgarone, Puget, and Perault 1992 and references given there),

estimation of the velocity correlation function and related 2-point statistics (see Hobson 1992, Kitamura et al. 1993, Miesch and Bally 1994 and references to earlier work given there) and searches for evidence of rotation (e.g. Goodman et al. 1994). Since one expects a signature of the dynamical and physical processes to appear in the velocity field, it is surprising and unfortunate that studies of this kind are not more prevalent. As a step toward a better understanding of molecular cloud velocity structure, Falgarone and coworkers (Falgarone 1989, Falgarone and Phillips 1990,1991, Falgarone et al. 1994; see below for discussion) have explicitly tried to relate radial velocity information to dynamical processes through the comparison of observed line profiles with frequency distributions, or probability distribution functions, found in experimental and simulation studies of turbulence. The present paper tries to extend that program to the frequency distribution of centroid velocities.

Recent work in several areas suggests that the one-point probability distribution function (pdf, or, loosely, the histogram) of dynamical variables like velocity is a useful tool that may be sensitive to dynamical processes. These studies include large scale structure of galaxy velocities (Bernardeau 1994, Korman et al. 1994, Catelan and Moscardini 1994), incompressible terrestrial turbulence (see below), distinguishing nonlinear chaotic processes from stochastic processes (Wright and Schult 1993), and characterization of samples of musical volume fluctuations (Scalo and Chappell 1995). In particular, studies of incompressible turbulence have shown that the higher moments (skewness, kurtosis,...) of the pdf can be used to constrain physical models for turbulent intermittency. For incompressible turbulence the pdf of the velocity field itself is very nearly Gaussian, at least on large enough scales (Batchelor 1953 and Monin and Yaglom 1971 review early work; see more recent experiments and simulations in Anselmet, Gagne, and Hopfinger 1984, Figure 1; Kida and Murakami 1989, Figure 6; Jayesh and Warhaft 1991, Figure 1; Chen et al. 1993, Figure 3.), although non-zero skewness must exist at some level in order to provide energy transfer among different scales. Non-Gaussian behavior is well-established for velocity *differences* at small scales and velocity *derivatives*, and there is strong evidence from experiments and simulations for non-Gaussian behavior in many other variables (see the papers referred to above and Chen et al. 1989, Castaing, Gagne and Hopfinger 1990, Vincent and Meneguzzi 1991, She et al. 1993). Often the pdf of the velocity difference or derivative field exhibits a near-exponential behavior at smaller and smaller scales, and much work has gone into understanding this behavior physically, especially in terms of the stretching properties of the advection operator (see She 1991 for a review). Part of the motivation of the present work is to investigate whether any of these properties occur in the more complex “turbulence” of interstellar clouds, and whether even the velocity fluctuation field itself presents measurable deviations from a Gaussian pdf.

Falgarone and Phillips (1990, 1991) have shown that line profiles constructed from high-sensitivity CO molecular line data (in several transitions) exhibit excess wing emission, relative to a single Gaussian, over a very large range of scales, from 0.02 to 450 pc . For all these line profiles the width of the wings is about 3 times the width of the line core if both are fit by Gaussians, but the fractional intensity of the wing component (fraction of mass at high velocities) varies between about 0.03 and 0.8. Broad wings were also found in high latitude molecular clouds by Magnani, Blitz and Wendel (1989). The presence of similar broad wings in regions whose scales are gravitating and non-self-gravitating, and in regions with and without internal massive star formation, suggests that the behavior is not due to stellar winds or collapse motions, and the variation in wing width in these regions seems to rule out a dilute warm gaseous component, as pointed out by Falgarone and Phillips. Since the line profile, in the optically thin case, is in effect a histogram of radial velocities, the broad wings have been viewed in the context of non-Gaussian pdfs, although there is some confusion concerning whether the line profile should be interpreted as the pdf of average line of sight velocities or of velocity differences; the latter interpretation is adopted by Falgarone and Phillips (1990) in comparisons with laboratory data.

A number of physically-based explanations for the broad wings have been proposed, as discussed by Falgarone et al. 1994 and in §4 below, but the systematics of non-Gaussian pdfs in star-forming regions have yet to be established. It is not even clear that line profiles give a valid representation of the pdf. Every line profile samples a line-of-sight velocity field which in general contains a component whose characteristic scale is a significant fraction of the sample depth. The form of these systematic line-of-sight motions is unknown and may severely limit the correspondence between the line profile and velocity pdf. Such problems can largely be circumvented in analyses of simulations, where it is possible to insure homogeneity on the largest scales (as in Falgarone et al. 1994), but homogeneity is probably not a good assumption in general for interstellar clouds. It is not difficult to show that the addition of a systematic component can significantly alter the estimate of the distribution of the velocity *fluctuations*, which is the function of interest. A cloud in non-solid-body rotation about its center, for example, will yield non-Gaussian line profiles along lines of sight displaced from the projection of the rotation axis onto the plane of the sky (provided this projection is nonzero). In particular, these profiles will exhibit apparent excess wing emission due solely to the *smearing* arising from the variation of the line-of-sight component of the rotational velocity with depth in the cloud, which will thus distort the pdf of velocity fluctuations. In addition, radiative transfer effects can distort emission lines and cause the wings to become relatively more prominent if the cloud is optically thick (although Falgarone & Phillips 1990 argue against this interpretation of the broad wings on the basis of their observed shapes).

An alternative procedure, which we adopt here, is to estimate the pdf of *centroid line velocities* (intensity weighted average velocity along the line of sight) sampled over a densely observed individual star formation region. While a “line profile” is a measure of the radial velocity (or velocity difference) pdf sampled along the line of sight, either in a single beam or averaged over many beams, the “centroid pdf” is the pdf of the mean velocity of line profiles taken over a large spatial sample of positions in the plane of the sky. The two functions differ in the direction along which the sampling for the pdf is taken, and in the quantity sampled. It follows from the central limit theorem that any deviations from Gaussian behavior in the centroid pdf implies the existence of higher-point spatial correlations in the velocity field, an interpretation which also applies to the line profile if it is viewed as an average over the beam. The advantages of the centroid pdf approach include the much lower sensitivity required for each of the individual line profiles and the weaker dependence of the results on large scale, systematic motions which, although still a concern, will tend to be mitigated by the line-of-sight averaging and by space filtering of the velocity maps (see below). For example, the centroid velocities of the rotating cloud discussed above will vary in an obvious way with position, and the effects of rotation can therefore be removed by applying an appropriate filter, a procedure which is not possible with the individual profiles unless the rotation curve of the cloud is known. In addition, the presence of a warm “interclump” medium, or of “optical depth broadening”, which would both contribute to the line profiles, will not much affect the pdf of centroid velocities, since the thermal component and the line saturation are symmetric (although the centroid pdf, in the optically thick case, would only sample fluctuations on the leading edge of the cloud). The problem with this approach is that the number of velocities (positions) which must be sampled in order to accurately estimate the tails of the pdf is very large, at least of order 1000. Furthermore, the relationship between the pdf of an average line-of-sight quantity (centroid velocity in this case) and the pdf of the radial velocity distribution in three dimensions is not clear; in the case of line profiles the third dimension is sampled, but the systematic motions in this dimension cannot be removed.

Work aimed at determining the pdf of interstellar gas motions based on centroid velocities dates back to the early 1950s. Several studies used optical absorption line velocities of “clouds” along the line of sight to relatively nearby OB stars (Blaauw 1952, Huang 1950, Kaplan 1954, Takakubo 1958, Munch

1957) and velocities of HI 21cm emission (Takakubo 1967, Mast and Goldstein 1970) and absorption (Crovisier 1978) lines to estimate the residual, or peculiar, velocity distribution, after correction for solar motion and differential galactic rotation. These studies all refer to fairly local gas, with distances less than about 500-1000 pc. In addition, Verschuur (1974) presented detailed HI emission mapping and “cloud” identification (from the spatial-velocity data cube) in two regions, one of which is suitable for estimation of the velocity pdf. In reading these studies, one finds either what the authors consider as clear evidence for non-Gaussian velocity distributions (Huang 1950, Blaauw 1952, Kaplan 1954, Munch 1957, Takakubo 1958, Mast and Goldstein 1970), with an exponential function giving a better fit to the pdfs, or a concern that systematic effects and small number statistics prevent a conclusion concerning the functional form of these distributions (Takakubo 1967, Crovisier 1978, Verschuur 1974). In no case does one find evidence supporting a Gaussian velocity distribution. However no theoretical explanation of these surprising results was forthcoming, and with the advent and subsequent prominence of molecular line observations, these studies were never repeated and were in effect forgotten. We know of no previous molecular line studies that have examined the centroid velocity pdf, that is, the histogram of centroid velocities sampled along many lines of sight.

The present Letter examines the frequency distribution of over 29,000 independent centroid radial velocities, divided between 12 star-forming regions and subregions, derived from the Bell Labs ^{13}CO (1-0) survey. We briefly discuss the data, present the pdfs estimated as histograms, estimate the skewness and kurtosis for each region, and briefly discuss the theoretical relevance of the results, as well as give a brief summary of theoretical models. A more complete presentation, including a discussion of the pdfs of velocity differences and linewidths, will be given elsewhere (Miesch and Scalo 1995, hereafter paper II).

2. Data

The data sets used here are the same as those used by Miesch & Bally (hereafter MB) in their study of the fluctuating, or “turbulent”, velocity structure in selected nearby molecular clouds as characterized by two-point statistical functions. The observations are of ^{13}CO J=1-0 emission in L1228, L1551, Mon R2, and Ori B as well as ^{13}CO J=2-1 observations of the molecular gas surrounding the Herbig-Haro object HH83 which lies in the Orion A cloud, just west of L1641 (Bally *et al.* 1994). We thank John Bally for making these data available to us for the present work. Notice that all of these regions and subregions are actively forming stars, as evidenced by observed outflows, HH objects, reflection nebulae, maser emission, probable T-Tauri and related stars, and high IR fluxes and point source counts as revealed by IRAS, and that energy input from these young stars has likely had a significant dynamical influence on the density and velocity structure of the clouds (Bally & Devine 1994; Bally, Castets, & Duvert 1994; Xie 1992; Pound & Bally 1991; Reipurth & Olberg 1991; Ogura & Sato 1990; Bally *et al.* 1989; Genzel & Stutzki 1989; Haikala & Laurejs 1989; see paper II for further discussion). In addition, external energy sources such as the OB associations in Orion (Genzel & Stutzki 1989) and the probable supernova remnant associated with L1228 (Grenier *et al.* 1989) could supply a significant amount of mechanical energy, both directly through transmitted shock waves (Miesch & Zweibel 1994) and ablation flows, and by induced star formation. The highly “stirred-up” nature of these regions is in contrast to some of the other regions in which broad emission line wings have been found (a quantitative measure of the relative star-forming activity of each region will be given in paper II).

All but the HH83 observations were made with the AT&T Bell Laboratories 7-m Crawford hill antenna

(with a beamwidth of $1'.7$ at 110 GHz) as part of the Bell Labs molecular cloud survey, while the HH83 data were obtained with the IRAM 30-m telescope on Pico Veleta, Spain (with a $0'.22$ beamwidth). The velocity resolution was 0.26 km s^{-1} for L1228, Mon R2, and Ori B, and 0.13 km s^{-1} for L1551 and HH83. Two regions in particular, Mon R2 and Ori B, were clearly composed of several distinct clouds, or subregions, (3 and 6 respectively) which were separated out in space and velocity prior to analysis (regions 1a, 1b, and 1c in Ori B are small clouds to the northeast of L1627, which lies in region 2. Region 4 is southwest of that, near the Horsehead Nebula and includes L1630, and region 3 spatially overlaps regions 2 and 4, but is at a significantly lower velocity).

The velocity centroid (defined as $\sum u_i T_i / \sum T_i$, where T_i and u_i are the brightness temperature and the velocity of the i^{th} channel and summation is over the line profile) was computed along each line of sight for which both the integrated intensity and the peak brightness temperature exceeded imposed threshold values, intended to minimize the influence of noise-dominated spectra. However it should be remembered in what follows that the pdfs are biased by what is probably a column density cutoff, as of course are all published descriptions of cloud structure. The data were oversampled by a factor of two when constructing the velocity centroid maps, so the actual number of independent spectra used for each of these regions is about a factor of four smaller than the total number of points in the map. This latter number (the number of points) is listed in Table 1 for each region we have studied, and varies from 822 to 21876. For further information on how the centroid velocity maps were constructed, and for a more detailed description of the observations themselves, see MB and the references given at the beginning of this section. Images of the velocity centroid structure will be presented in paper II.

We are interested here in single-point statistics describing the fluctuating velocity structure in star-forming regions, and we have therefore filtered out large scale, systematic motions such as velocity gradients across the maps by first convolving the raw data with a suitable smoothing function (either a Zurflueh or moving average filter; see MB for a detailed discussion of the filtering process) and then subtracting the smoothed map from the original to obtain the fluctuating velocity component. The width of each smoothing function (which is roughly equal to the cutoff wavelength of the high-pass filtering process) was chosen to be the largest value at which asymmetric lobes (which are the signature of large-scale gradients) were no longer discernible in the autocorrelation function of the residual centroid map. The ratio of the effective scale of the observations (taken to be the square root of the total number of points) to the filter size is given in Table 1 for each region. The unfiltered probability density functions were usually significantly different than the filter-subtracted versions, the former showing multimodal behavior and large asymmetries. This illustrates the danger of estimating pdfs (or any statistical descriptor) from data that contain structure whose scale is a significant fraction of the mapped region, and also suggests, as mentioned earlier, that spectral line profiles may not give a valid representation of the velocity fluctuation pdf, since there is no way to filter out the line-of-sight systematic component. Indeed, the average line profiles of these regions exhibit a variety of forms that suggest systematic large scale structure along the line of sight (Miesch and Scalo 1995).

3. Analysis and Results

Histograms (hereafter probability density functions or pdfs) of the centroid velocities for each of the 12 regions we have studied are exhibited in Figure 1, normalized with respect to the total number of points in each map. The plots are log-linear, so a Gaussian will appear as a parabola while an exponential will

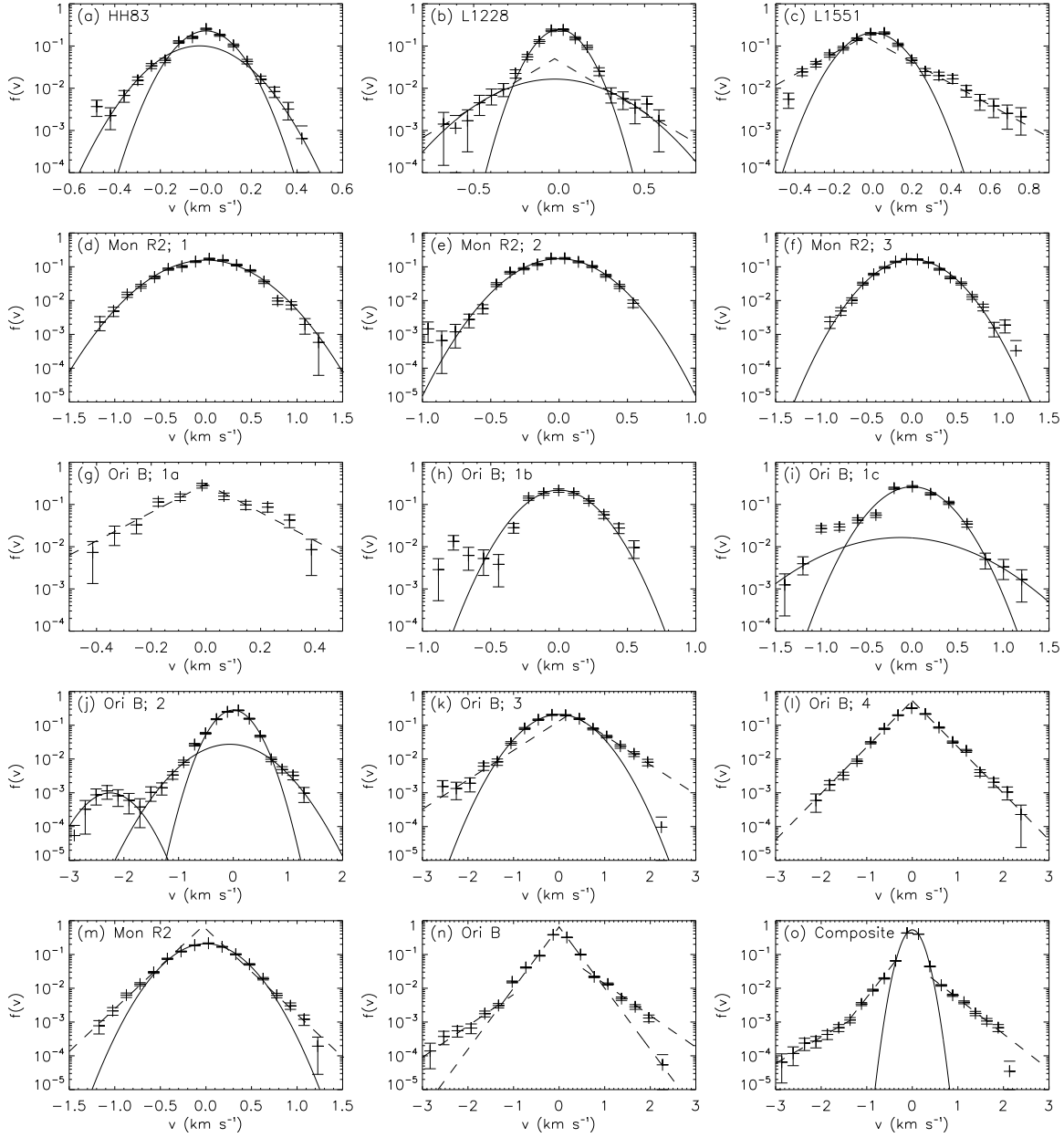


Fig. 1.— Probability distribution functions of the observed centroid velocities, including both histograms (crosses, with statistical error bars) and functional fits (lines), the latter of which take two forms: Gaussian ($f(v) = f_* e^{-(v-v_*)^2/2\sigma_*^2}$; solid lines) and exponential ($f(v) = f_* e^{-\sqrt{2}|v-v_*|/\sigma_*}$; dashed lines). Each region is labeled and the final three frames represent the normalized pdfs averaged over the three Mon R2 regions (m), the six Ori B regions (n), and all 12 data sets (o). Note that, for the linear-logarithmic axes chosen, an exponential takes the form of a straight line and a Gaussian a parabola. The anomalously low point in the high velocity tail of Ori B, region 3 (k), which is reflected in the composites (n) and (o), is probably an artifact, as explained in the text.

Table 1
PDF Attributes ^a

Region	No. of points ^b	Filtering Ratio	Core Fraction	Dispersion	Skewness	Kurtosis	
	N	\sqrt{N}/ℓ_f	(percent)	σ ($km\ s^{-1}$)	ξ	κ	
HH83	6235	2.4	91 (85)	0.12 (0.12)	-0.62 (-0.53)	4.2 (3.9)	
L1228 ^c	3532	3.5	96 (94,95)	0.14 (0.15, 0.14)	-0.20 (-0.33, -0.31)	5.9 (12, 7.4)	
L1551	4726	2.7	79 (71)	0.18 (0.22)	0.65 (-0.54)	4.6 (7.0)	
Mon R2	1	8630	2.3	100 (100)	0.37 (0.38)	-0.14 (0.00)	3.0 (3.0)
	2	7592	2.1	100 (100)	0.23 (0.23)	-0.37 (0.00)	3.2 (3.0)
	3	12208	2.7	100 (100)	0.29 (0.29)	0.054 (0.00)	3.2 (3.0)
Ori B	1a	822	1.4	100 (100)	0.15 (0.18)	0.13 (0.00)	3.0 (6.0)
	1b	2094	2.2	97 (100)	0.22 (0.20)	-0.60 (0.00)	4.8 (3.0)
	1c	4801	3.3	89 (97)	0.37 (0.33)	-0.86 (-0.46)	4.2 (5.7)
	2 ^d	18420	3.3	97 (96,96)	0.35 (0.35, 0.31)	-1.5 (-1.4, -0.28)	11 (12, 5.2)
	3	10433	2.0	90 (83)	0.64 (0.69)	0.54 ^e (0.73)	3.9 (5.6)
	4	21876	2.9	100 (100)	0.47 (0.45)	0.19 (0.00)	4.8 (6.0)

^aThe values without and within parentheses are obtained respectively by discrete summations using the observed histograms, and by integration using the piecewise smooth analytic fits described in the text and shown in Fig. 1

^bThe actual number of spectra used is roughly one fourth these values because the maps were oversampled by a factor of two (see text).

^cThe two analytic values are for exponential and Gaussian wings respectively (see Fig. 1b).

^dThe latter analytic value excludes the component centered at $-2.25\ km\ s^{-1}$.

^eThe skewness calculated directly from the data points excludes all points for which $|v| \gtrsim 2.2\ km\ s^{-1}$ (see text).

appear linear. Also included are composite histograms made by averaging the normalized pdfs for the three Mon R2 regions (Figure 2m), for the six Ori B regions (Figure 2n), and for all 12 data sets (Figure 2o), intended in some sense to approximate ensemble averages (provided similar physical processes are occurring in each region). Observed values are shown as crosses, with vertical error bars representing the statistical uncertainty in each bin, which we have taken to be $\epsilon_i = 2\sqrt{N_i}/N$, where N_i is the number of events in the bin and $N = \sum_i N_i$ is the total number of points in the map. The denominator in this expression for ϵ_i arises from the normalization chosen and the factor of 2 is present because, as mentioned above, these maps have been oversampled, so the actual number of independent spectra is about one fourth the number of points, both in the map as a whole and in the individual bins. Overlaid on the data of Figure 1 are several functional fits to each of the pdfs, having either Gaussian (solid lines) or exponential (dashed lines) forms (more general forms will be considered in paper II). The horizontal axes in each frame of Figure 1 have been adjusted so that $v = 0$ corresponds to the center of the fitted primary (core) component. Table 1 includes the fraction of the total area under each pdf curve due only to the core component, expressed as a percentage. Results for Ori B, region 2 are listed both with and without the secondary component centered at a relative velocity of $-2.25\ km\ s^{-1}$ because this component is likely due to residual emission from region 3, which lies in the same area of the sky but at a lower velocity.

A useful way to quantify the shape of probability density functions which has been used extensively in the study of intermittency in incompressible turbulence (e.g. Monin & Yaglom 1971; Vincent & Meneguzzi

1991) is by means of n^{th} order moments which, for a pdf $f(v)$, are given by

$$\mathcal{M}^{(n)} \equiv \frac{\int_{-\infty}^{\infty} v^n f(v) dv}{\int_{-\infty}^{\infty} f(v) dv}. \quad (1)$$

We then define the dispersion, or standard deviation, σ , the skewness, ξ , and the kurtosis, or flatness factor, κ , in terms of the second, third, and fourth moments:

$$\sigma \equiv \sqrt{\mathcal{M}^{(2)}}, \quad \xi \equiv \frac{\mathcal{M}^{(3)}}{\sigma^3}, \quad \text{and} \quad \kappa \equiv \frac{\mathcal{M}^{(4)}}{\sigma^4}. \quad (2)$$

The units of σ are those of velocity, while ξ and κ are dimensionless. Table 1 contains the values of σ , ξ , and κ for each region, including both results obtained from the observed histograms using a discrete summation analogous to equation (1) and those obtained by analytically integrating the functional fits using the forms and parameters shown in Figure 1. For those pdfs which appear to be composed of more than one component, we have adopted a piece-wise smooth representation which changes character discontinuously where the tail and core fits intersect. When the fits are adjusted to avoid discontinuities in the first derivative, the resulting changes in the moments of Table 1 are minimal (if the smoothing scale at each discontinuity is the size of a bin, these changes do not exceed 4%).

The composite regions have been omitted from Table 1 because some quantitative results (e.g. excessively large values of the kurtosis) arise simply as a result of averaging (or equivalently, summing) a small number of normalized pdfs with different dispersions, and they are therefore not useful diagnostics of the flow fields (although the integral over a large number of Gaussian pdfs with fluctuating dispersions has been used by Castaing et al. 1990 to study velocity difference pdfs). However, we do not see how this averaging could give rise to the exponential tails so prevalent in all of the composite pdfs, so we must regard their general functional forms to be a result of physical processes, and as such, to be of interest. The skewness of the composites is also of interest and, when calculated using the discrete data points, is found to be -0.17 for Mon R2, 0.22 for Ori B, and 0.16 for the “all regions” composite (note that, in calculating the moments for the latter two, the anomalously low point at $v \sim 2.2 \text{ km s}^{-1}$ was excluded from the summations, as well as all points with a velocity less than $v \lesssim -2.2 \text{ km s}^{-1}$, in order to minimize the influence of the sharp cutoff at high velocities, which is probably spurious; see below). The corresponding values using the analytic fits are -0.19, 0.66, and -0.11 (the large discrepancy for the latter two can be attributed to the spurious cutoff, which greatly influences the values obtained directly from the data but does not appear in the fits).

Before proceeding, we emphasize that the fits considered here are primarily included only for comparison and to provide an alternative method for approximating the histogram moments. They are not intended to be unique descriptors of the true form of the underlying pdfs. On a related note, we also stress that the fitted moments listed in Table 1 are only approximate and are sensitive to the form of the fitting function. For example, the kurtosis of the L1228 pdf varies by 62% depending on whether the tails are taken to be exponential or Gaussian (Table 1). The statistics in the far tails, which give a significant contribution to the high-order moments, are simply not good enough in most cases to make a unique, unambiguous identification and extrapolation, even if the pdfs were truly well described by simple functional forms. Also, the uncertainty in each centroid velocity arising from instrumental noise can distort the pdfs, leading to an increase in the effective histogram bin size due to the “spillover” from neighboring bins. A complete treatment of this effect will be deferred to a later paper (paper II), but for now we note that the influence of this “spillover” on the values of the skewness and kurtosis has been estimated and is found to be typically less than 20% (but possibly up to 50%, with the largest discrepancies occurring in L1228 and Ori B, region

2). It should also be pointed out that other methods of pdf estimation, such as kernel and parametric estimators (Vio *et al.* 1994), may be preferable to the classical histogram estimator used here.

Despite these difficulties and qualifications, it is evident that many of the pdfs shown in Figure 1 exhibit broad, often nearly exponential, tails indicative of highly non-Gaussian fluctuating velocity structure. In particular, there is good evidence for nearly exponential behavior in the tails of all of the composite spectra, along with L1551, Ori B regions 3 and 4, and possibly L1228 and Ori B region 1a, although the latter is questionable (recall that this region, Ori B 1a, is the smallest of the data sets, composed of only several hundred independent spectra). Secondary tail components with a steeper behavior, approaching Gaussian, may be present in HH83, Ori B region 2, and possibly L1228 and Ori B region 1c, although again, the latter has both the largest discrepancy and the poorest statistics. Note that the sharp cutoff at $v \sim 2.2 km s^{-1}$ in Ori B, region 3 (Fig. 1k), and in the Ori B and all regions composites (Figs. 1n and o), which are dominated by this region at high velocities, are likely an artifact of the manner in which the centroid velocities for this region were computed. As mentioned above, region 3 overlaps regions 2 and 4 in space but lies at a lower velocity, and in order to isolate the emission from this region, it was necessary to sum over only part of the profile, cutting off at high velocities to avoid contributions (and subsequent biasing of the centroid velocity) from the other components. Two upper cutoffs were used for the calculation of the centroid velocity (see MB), the first (used for 60% of the points) was $9.2 km s^{-1}$ (lsr) and the second (including the remaining 40%) was $7.5 km s^{-1}$ (lsr). Since the horizontal axis of Fig. 1(k) is centered about an lsr velocity of $5.04 km s^{-1}$, then it is likely that the high velocity cutoff in the pdf at $2.2 km s^{-1}$ (which translates to about $7.2 km s^{-1}$ lsr) is due to the high velocity cutoff in the calculation of the centroids and not to any sharp variation in the true pdf. We have taken this cutoff into account when calculating the skewness of Ori B, region 3, and the Ori B and “all regions” composites by excluding all points with velocities $|v| \gtrsim 2.2 km s^{-1}$, which included the anomalously low point at the high velocity end and several (2 to 4) points on the low velocity end, so that the pdfs would not be biased toward low velocities. The remaining entries in Table 1 for Ori B, region 3, however, were calculated using the full histogram.

The often negative (but fairly well distributed) skewnesses of the centroid pdfs are in contrast to the positive values typically seen in the average line profiles for each region, which, particularly in the cases of HH83, L1551, and L1228, show some excess blue-shifted emission likely due to molecular outflows whose red-shifted lobes are partially shrouded or otherwise absent. This suggests again that the line-of-sight averaging and the space filtering inherent in the centroid pdf approach make it less sensitive to systematic motions (such as outflow bubbles) than are individual or average profiles for the same region.

It is interesting to compare the pdfs of Figure 1 with the line profiles observed by Falgarone & Phillips (1990), which sample radial velocity fluctuations along the line of sight and which exhibit relatively broad wings. In order to quantify the excess wing emission, they fit their observed profiles to two separate Gaussian components. Falgarone and Phillips were primarily interested in demonstrating the similar core/wing scaling on very different scales, and so were careful not to draw conclusions about the shapes of the wings, although they remark that most of the profiles were better fit with two Gaussians, and in only a few cases were better fit with exponential or Lorentzian wings. For the two-Gaussian fits, they find typical dispersion ratios (wing/core, hereafter D) of 3.3 ± 0.2 and amplitude ratios (wing/core, hereafter P) ranging between about 0.03 and 0.8. The sum of two centered Gaussians with these values for P and D give kurtoses between 3.9 and 10.2, a range that is higher than most of the values listed in Table 1. Of the pdfs in Figure 1 which show an approximately Gaussian secondary component, the corresponding ratios are: $D = 1.45$ and $P = 0.44$ for HH83, $D = 2.5$ and $P = 0.067$ for L1228, $D = 2.1$ and $P = 0.063$ for Ori B region 1c, and $D = 1.9$ and $P = 0.097$ for the two strongest components in Ori B region 2.

The somewhat smaller kurtoses and dispersion ratios in the present work (despite the much less quiescent nature of the regions we have studied) may in part be a result of the line-of-sight averaging inherent in the centroid pdf approach, which will tend to make the distribution more Gaussian if the velocity structure is indeed stochastic (this follows from the central limit theorem). It is also possible in principle that the larger values of D found for the individual profiles could be due in part to a warmer, more rarefied molecular “inter-clump” medium, which would be apparent in the profiles (provided the column density is sufficient), but, due to its symmetry, would not show up in the centroid velocity measurements. Thus, the core fraction in the centroid pdfs (Table 1) relative to that observed in individual or average profiles can be used to set column density limits on such a warm, molecular medium, if the cloud and its surrounding medium are optically thin. Also, as mentioned above, “optical depth broadening” could give rise to excess wing emission that would have no counterpart in the centroid pdfs. However, as noted by Falgarone and Phillips (1990), the line shapes, at least for their data, seem to rule out optical depth effects, and the variation among the wing dispersions make it unlikely that warm gas is a dominant component.

4. Comparison with Theory

A number of theoretical models provide mechanisms to produce broad tail components in the velocity pdfs, although none of them explain why the tails are nearly exponential in some regions, as found here. Collisions of clouds (Keto and Lattanzio 1989) or gas oscillations and streams connected with clumps which might represent non-linear waves or other phenomena (Elmegreen 1990, 1994) produce a “core-envelope” density structure with distinct velocity distributions. Greaves and White (1991) have interpreted a velocity discontinuity in the OMC1 ridge as evidence for such a collision. Elmegreen’s model assumes that the gas is composed of unresolved clumps with intrinsic velocity distributions in both the core and envelope regions that are Gaussian from locally randomized motions and clump-clump interactions according to the central limit theorem, with superimposed streaming motions from non-linear waves. By further assuming that the streaming part has a power law velocity-density scaling similar to that expected for non-linear MHD waves and related processes (Adams and Fatuzzo 1993), Elmegreen (1990) showed that the resulting composite velocity distribution, integrated over the density gradient along the line of flow symmetry and *inside* a single beam or averaged over over many beams, agrees well with the broad wing profiles observed by Falgarone and Phillips (1990), including the universal 3:1 wing:core dispersion ratio obtained from a two-Gaussian fit. Elmegreen (1994) discussed how the relative strengths of the core and wing might depend on time. The kurtoses of these pdfs (Elmegreen, personal communication) span the range found in the present work, varying with the assumed density contrast and relative amplitudes of the core and envelope. However the correspondence between this integral average along the density gradient and the spatially sampled centroid pdf investigated here is unclear – primarily because the pdf of the model depends on how well the streaming motions and clump-clump dispersions are resolved. The spatial pdf of *resolved* clumps and flows will depend on spatial orientation and other parameters; presumably a smooth and symmetric centroid-pdf comparable to those observed here will result from an average over a large number of lines of sight, if the scale of these motions is still much smaller than the scale of the sampled region. If the clumps are *unresolved*, then the envelopes will only contribute to the average spectral line wings (which will be broad) but not to the centroid velocity *within* a single beam; this will produce a centroid pdf that is just determined by the motions of the core regions. The best agreement between the models and the observations arises if the colliding flows (or some of them) are resolved; then the velocity distribution for all of the pieces of the flow

will produce broad tails on the centroid pdf instead of broad linewings on the individual spectra. With only partial resolution, both the centroid pdf and the individual spectra will have broad tails or wings.

The structures found by Keto and Lattanzio (1989) are the result of 3-dimensional hydrodynamic simulations of cloud collisions. Their Figures 4-6 are images of the velocity centroids that are directly comparable with the observed centroid images used here, although the pdfs were not presented. (Keto and Lattanzio *do* give a montage of line profiles along individual lines of sight, which show a great variety of shapes.) However, because the flows are not assumed to be unresolved, and because the wing emission is due to the streaming motion of the envelope (rather than the dispersion of the clumps posited by Elmegreen), the velocity field will depend on initial conditions, time, and especially viewing angle. An average over these parameters would be necessary to compare with the densely sampled regions studied here, which are likely to include a number of such single-event collisions. It might be possible to obtain flat (relative to a Gaussian) wings in the cloud collision model if the inflowing material has, say, a power-law velocity profile as a function of distance from the compressed layer, but we have insufficient data from the simulations to check this. Hopefully future simulations will provide the necessary information.

Rather than attribute the pdf tails to such highly compressible collisions or streams, another possibility is that the pdf tails are due to an excess of high-velocity events evoked by the vortical part of the advection operator, which causes the velocity derivative and dissipation field to become highly localized (e.g. in vorticity tubes in 3D incompressible turbulence). This process, often referred to as “intermittency” because a stationary probe in the flow records a “bursty” velocity time series as the high-intensity patches flow by, is the explanation favored by Falgarone and Phillips, although they were referring to the pdf of velocity differences or derivatives, not the velocity itself (we note again the problem with interpreting the line profile as a pdf of velocity *differences*). However it is known from turbulence simulations that even purely incompressible nonlinear advection (in concert with pressure gradients) can produce broad velocity pdf tails at small enough scales, especially in the dissipation range (e.g. Yamamoto and Kambe 1991, Fig.1) and at not-so-small scales in convective MHD turbulence at low Mach numbers (Brandenburg et al. 1994), although the latter may include other effects arising from magnetic fields and rotation. These studies suggest that even in the compressible, self-gravitating case nonlinear advection may play a major role. In this regard the low-resolution (20x20) 2-dimensional simulations of rotating self-gravitating, compressible turbulence (a magnetic field was *only* included by taking a polytropic index of 2) by Yue et al. (1993) are of interest. These calculations give broad wings similar to the observations of Falgarone and Phillips; given the low resolution, it is unlikely that cloud or stream collisions could play a role, so perhaps nonlinear advection coupled with gravity (and possibly rotation) is all that is required. The advective effects cannot be due to the usual association of intermittency with vorticity stretching, though, since this term does not exist in two dimensions. The very low resolution is of concern, however, as well as the possible dependence on the imposed symmetry assumptions and unusual initial conditions. Again there is no indication of how these simulations can account for the nearly exponential wings or the *variations* in the observed pdfs (e.g. some are nearly Gaussian).

Concerning the importance of magnetic effects in contributing to broad pdf tails, we know of only two relevant results. First, the simulation of hydrodynamic particles with imposed wave forcing meant to represent magnetic fields by Stenholm and Pudritz (1993), do *not* show any excess wings in line profiles, although it may be argued that this is not really an MHD simulation, since the waves are simply imposed on the gas with some frequency and amplitude. On the other hand, the simulations of 3-D, rotating, thermally forced MHD turbulence by Brandenburg et al. (1994) do exhibit broad tails in the *velocity* pdfs, at least in the horizontal directions (the pdf of vertical velocity is dominated by convective motions such

as updrafts and plumes and is therefore not as directly comparable to the present results, which are for velocity *fluctuations*).

Higher-resolution (512^3) 3-dimensional simulations of decaying compressible turbulence (without self-gravity or magnetic fields) have been performed by Porter, Pouquet, and Woodward (1993), and Falgarone et al. (1994) present centroid velocity pdfs for individual 32×32 subregions. This is just the type of analysis that is needed for a comparison with line shapes or pdf forms. The pdfs of the subregions show a wide variation in appearance, and, in particular, kurtosis (Lis, personal communication), but these are dominated by coherent motions on the scale of the subregions or larger. When the entire simulation box is included, the velocity pdf is nearly Gaussian. These simulations may be applicable to some quiescent clouds, but since they do not include self-gravity or internal stellar sources of energy input, they are not directly comparable to the observations of active regions presented here.

We expect that the influence of internal star formation is crucial in understanding the observed pdfs of active regions. Two-dimensional simulations including heating or stirring by star formation and cooling have been given by several groups (see Bania and Lyon 1980, Balsler, Bania, and Lyon 1990, Rosen, Bregman, and Norman 1993, Vazquez-Semadeni, Passot, and Pouquet 1994). These simulations variously include self-gravity (Vazquez-Semadeni et al.), radiative transfer and ionization (Bania et al. group), and the stellar component as a fluid (Rosen et al.), but the important point in common is the inclusion of energy and momentum input due to young massive stars, whose formation rate is parameterized in terms of some assumed dependence on the density and perhaps other variables. Unfortunately, a velocity pdf analysis of the type provided by Falgarone et al. (1994) is unavailable for these simulations. The present work suggests that the ability of these models to yield a range of velocity pdfs from nearly Gaussian to Gaussian cores with nearly exponential tails, will provide a critical test of the models, although it must be again remembered that in two dimensions vorticity stretching is absent; the importance of vorticity stretching might be implicated by the absence of exponential wings in 2-dimensional simulations that include much of the otherwise important physics (Vazquez-Semadeni, personal communication). Preliminary work on the velocity pdfs of the simulations of Vazquez-Semadeni et al. is underway.

Although collisions, nonlinear advection, and star formation activity all suggest themselves as explanations of the broad tails, it is clear after some thought that in an active star-forming region these three processes cannot be separated; for example, stellar winds and ionization drive flows that cause collisions which may form more stars, etc. For this reason it appears that careful analysis of numerical simulations afford the best theoretical approach to understanding the observed phenomena of broad pdf velocity tails. In the meantime, we can find no theoretical model that explains why the tails would be nearly exponential, Perhaps a mapping model of the advection term similar to that discussed by, e.g. She et al. (1993), but generalized to the compressible or even magnetized case will be useful.

In summary, we have investigated the fluctuating velocity structure in several nearby molecular clouds using the probability distribution function of emission line centroid velocities and we find evidence for non-Gaussian behavior in most of the regions we have studied. The most important results seem to be the variation between subregions, and the nearly exponential tails found in several cases. Although several theoretical interpretations have been discussed, in most cases the theoretical data is insufficient for a comparison with these observations, although we have found no explanation for the nearly exponential tails.

We would like to thank John Bally again for providing the data sets used in this work and for countless discussions regarding their analysis and interpretation. Bruce Elmegreen, Darek Lis and Enrique

Vazquez-Semadini kindly provided data on the pdf moments for their models. We thank Edith Falgarone and Bruce Elmegreen for comments on an earlier version of this manuscript. MSM would also like to thank Ellen Zweibel and Juri Toomre for their insight, encouragement, and financial support.

REFERENCES

- Adams, F.C. and Fatuzzo, M. 1993, *ApJ*, 403, 142
- Anselmet, F., Gagne, Y., and Hopfinger, E.J. 1984, *J.Fluid Mech.*, 140, 63.
- Bally, J., & Devine, D. 1994, in preparation
- Bally, J., Castets, A., & Duvert, G. 1994, *ApJ*, 423, 310
- Bally, J., Stark, A., Wilson, R. W., and Langer, W. D. 1989 in *The Physics and Chemistry of Molecular Clouds*, ed. Winnewisser, G. & Armstrong, J. T. (Berlin: Springer-Verlag) p. 81
- Balser, D.X., Bania, T.M., and Lyon, J.G. 1990, in *The Formation and Evolution of Star Clusters*, ed. K.Janes (San Francisco: Ast.Soc.Pacific), p.136.
- Bania, T.M. and Lyon, J.G. 1980, *Ap.J.*, 239, 173.
- Bernardeau, F. 1994, *Ap.J.*, in press.
- Brandenburg, A., Jennings, R. L., Nordlund, A., Rieutord, M., Stein, R.F., & Tuominen, I. 1994, *J. Fluid Mech.*, in press
- Castaing, B., Gagne, Y., and Hopfinger, E.J. 1990, *Physica D* 46, 177.
- Catelan, P. and Moscardini, L. 1994, preprint.
- Chappell, D. and Scalo, J. 1995, in press
- Chen, H., Herring, J.R., Kerr, R.M., and Kraichnan, R.H. 1989, *Phys.Fluids A* 1, 1844.
- Chen, S., Doolen, G., Herring, J.R., Kraichnan, R.H., Orszag, S.A., & She, Z.S. 1993, *Phys.Rev.Lett.* 70, 3051.
- Crovisier, J. 1978, *A&A*, 70, 43.
- Elmegreen, B. G. 1990, *ApJ*, 361, L77
- Elmegreen, B. G. 1994, in *First Symposium on Infrared Cirrus and Interstellar Diffuse Clouds*, ed. Roc Cutri and Bill Latter, *Astronomical Society of the Pacific Conference Series*, Volume 58, page 380-395.
- Falgarone, E., Lis, D.C., Phillips, T.G., Pouquet, A., Porter, D.H., and Woodward, P.R. 1994, preprint.
- Falgarone, E. & Phillips, T.G. 1990, *Ap.J.* 359, 344.
- Falgarone, E. & Phillips, T.G. 1991, in *Fragmentation of Molecular Clouds and Star Formation*, ed. E. Falgarone et al., p.119.
- Falgarone, E. Puget, J.-L., and Perault, M. 1992, *Astr.Ap.* 257, 715.
- Greaves, J.S. and White, G.J. 1991, *Astr.Ap.*, 248, L27.
- Houlahan, P. and Scalo, J. 1992, *ApJ*, 393, 172
- Jayesh and Warhaft, Z. 1991, *Phys.Rev.Lett.* 67, 3503.
- Kida, S. and Murakami, Y. 1989, *Fluid Dyn. Res.* 4, 347.
- Keto, E.R. and Lattanzio, J.C. 1989, *Ap.J.*, 346, 184.
- Korman, L., Bertschinger, E., Gelb, J.M., Nusser, A. and Dekel, A. 1994, *Ap.J.*, in press.
- Magnani, L., Blitz, L., and Wendel, A. 1988, *Ap.J.* (Letters), 331, L127.
- Miesch, M. S. & Bally, J. 1994, *ApJ*, 429, 645
- Miesch, M. S. & Scalo, J. 1995, in preparation
- Miesch, M. S. & Zweibel, E. G. 1994, *ApJ*, 432, 622
- Monin, A. and Yaglom, A. 1971, *Statistical Fluid Dynamics* (Cambridge: MIT Press).
- Pound, M. W. & Bally, J. 1991, *ApJ*, 383, 705
- Porter, D.H., Pouquet, A., and Woodward, P.R. 1993, *Theor. Comp. Fluid Dynamics*, 4, 13
- Rosen, A., Bregman, J.N., and Norman, M.L., 1993, *Ap.J.*, 413, 137.
- Scalo, J.M. 1990, in “Physical Processes in Fragmentation and Star Formation”, ed. R. Capuzzo-Dolcetta, C.Chiosi, and A. Di Fazio (Dordrecht:Kluwer), p.151.
- Scalo, J. and Chappell, D. 1995, in preparation
- She, Z.-S. 1991, *Fluid Dyn.Res.* 8, 143.
- She, Z.-S., Chen, S., Doolen, G., Kraichnan, R.H., and Orszag, S.A. 1993, *Phys.Rev.Lett.* 70, 3251.
- Stenholm, L.G. and Pudritz, R.E. 1993, *Ap.J.* 416, 218
- Vazquez-Semadeni, E., Passot, T., and Pouquet, A. 1994, *Ap.J.*, in press.
- Vincent, A. and Meneguzzi, M. 1991, *J.Fluid Mech.* 225, 1.
- Wright, J. and Schult, R.L. 1993, *Chaos* 3, 295.
- Yamamoto, K. and Kambe, T. 1991, *Fluid Dyn. Research* 8, 65.
- Yue, Z.Y., Zhang, B., Winnewisser, G., and Stutzki, J. 1993, *Ann.Physik* 2, 9.
- Zimmermann, T. and Stutzki, J. 1994, *Fractals*, in press.